



# Preparation and gas-sensing performance of $\text{In}_2\text{O}_3$ porous nanoplatelets

Lijun Guo<sup>a</sup>, Xiaoping Shen<sup>a,\*</sup>, Guoxing Zhu<sup>a</sup>, Kangmin Chen<sup>b</sup>

<sup>a</sup> School of Chemistry and Chemical Engineering, Jiangsu University, Zhenjiang 212013, PR China

<sup>b</sup> School of Materials Science and Engineering, Jiangsu University, Zhenjiang 212013, PR China

## ARTICLE INFO

### Article history:

Received 23 September 2010

Received in revised form 10 January 2011

Accepted 24 January 2011

Available online 1 February 2011

### Keywords:

Indium oxide

Nanoplatelets

Ethanol

Gas sensing

Sensor

## ABSTRACT

$\text{In}_2\text{O}_3$  porous nanoplatelets were successfully synthesized by solvothermal treatment of indium acetylacetonate, followed by calcination in air. X-ray diffraction and Raman spectrum measurements demonstrate that the products are pure cubic phase  $\text{In}_2\text{O}_3$ . Scanning electron microscopy and transmission electron microscopy analyses reveal that the  $\text{In}_2\text{O}_3$  nanoplatelets bounded by  $\{110\}$  planes with thickness less than 6 nm and length about 20–50 nm are single crystalline but with porous structure. The optical absorption property of the  $\text{In}_2\text{O}_3$  nanoplatelets was investigated by UV–vis spectroscopy, which indicates that the  $\text{In}_2\text{O}_3$  nanoplatelets are semiconducting with a direct band gap of 3.1 eV. The gas sensing performance of the as-prepared  $\text{In}_2\text{O}_3$  porous nanoplatelets was investigated towards a series of typical organic solvents and fuels. It was found that the  $\text{In}_2\text{O}_3$  porous nanoplatelets show structure-induced enhancement of gas sensing performance, and especially possess high sensitivity and rapid response towards ethanol vapor.

© 2011 Elsevier B.V. All rights reserved.

## 1. Introduction

Gas sensors have a wide application in the fields such as environmental monitoring, industrial production, domestic safety, and public security for their detection of combustible and noxious gases in the air [1–3]. Metal oxide nanostructure-based gas sensors have attracted much attention owing to their low manufacturing cost, low operation power consumption, simple design, and high compatibility with microelectronic processing.

For an  $n$ -type oxide semiconductor, intrinsic oxygen vacancies are responsible for its electronic conductivity. The adsorption of oxidative gas species will create extrinsic surface acceptor states that repel conduction band electrons, which results in lower conductivity, while reductive gas will cause reverse result. Therefore, the gases can be detected through monitoring the change of electronic conduction. Most of the present effort is being contributed to the improvement of sensitivity, selectivity, and long term stability of gas sensors. For a high sensitivity (i.e., great change in conductivity) and a fast response rate, the sensing material should exhibit large surface areas, and allow for good accessibility of the sensing material surface. To fulfill these requirements for gas sensors, one method is to decrease the size of sensor material, or to prepare porous structure for increasing the surface-to-volume ratio. Another route is to design and synthesize the nanostructure of sensing material exposing unique lattice planes [4], which would have stronger or selective absorption ability for detecting gases.

$\text{In}_2\text{O}_3$  is an important  $n$ -type transparent conductive semiconductor with a wide band gap, and holds promising applications in optoelectronic device such as UV lasers, gas sensors, solar cells, flat-panel displays, and so forth [5–8].  $\text{In}_2\text{O}_3$  nanostructures have been proven to be a highly sensitive material for the detection of both reducing and oxidizing gases [9]. During recent years,  $\text{In}_2\text{O}_3$  nanostructures with various morphologies and sizes have been developed, such as nanoparticles (cubes, octahedrons, and pyramids) [10], nanowires [11], nanorods [12], nanobelts [13], ultrathin corundum-type  $\text{In}_2\text{O}_3$  nanotubes [14],  $\text{In}_2\text{O}_3$  nanotubes filled with In [15], and  $\text{In}_2\text{O}_3$  nanocrystal chains and nanowire networks [16].

However, to the best of our knowledge, the two-dimensional  $\text{In}_2\text{O}_3$  nanostructures such as nanoplatelets have not been reported until now. Herein,  $\text{In}_2\text{O}_3$  nanoplatelets are prepared through a precursor route mediated by  $\text{In}(\text{OH})_3$ . The obtained  $\text{In}_2\text{O}_3$  nanoplatelets bound by  $\{110\}$  lattice planes show a single crystalline nature but with porous structure feature. Importantly, benefited from the porous structure, small size, and probably the unique surface lattice plane, the as-prepared  $\text{In}_2\text{O}_3$  nanoplatelets show excellent gas sensing performance towards a series of typical organic solvents and fuel vapors.

## 2. Experimental

### 2.1. Chemicals

All the chemical reagents used in our research are of analytical grade and are used without further purification. The molecular precursor, indium acetylacetonate [ $\text{In}(\text{acac})_3$ ], was synthesized according to the literature method [17].

\* Corresponding author. Tel.: +86 511 84401889; fax: +86 511 88791800.  
E-mail address: [xiaopingshen@163.com](mailto:xiaopingshen@163.com) (X. Shen).

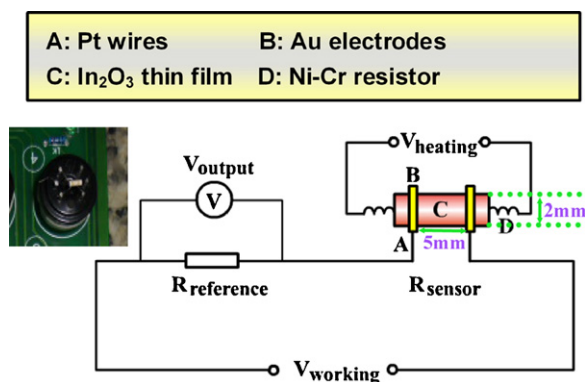


**Fig. 1.** Schematic illustration of the gas sensor measurement system together with a digital picture of the gas sensor. The reference resistor is 200 k $\Omega$  and the  $V_{\text{working}}$  is 5 V in the test.

## 2.2. Synthesis of $\text{In}_2\text{O}_3$ porous nanoplatelets

In a typical procedure for synthesizing  $\text{In}_2\text{O}_3$  porous nanoplatelets, the molecular precursor of  $\text{In}(\text{acac})_3$  (0.10 g) and a surfactant of sodium dodecyl sulfate (SDS, 0.08 g) were dissolved into 20 ml of ethylene glycol with strongly stirring. The mixture was then sealed into a 30 ml Teflon-lined stainless steel autoclave. The autoclave was maintained at 180 °C for 12 h, and then was allowed to cool to room temperature naturally. The as-formed precipitate was separated by centrifugation, washed with distilled water and ethanol several times, and dried in vacuum at 60 °C for 3 h. The obtained products were further calcinated in air at 350 °C for 3 h and  $\text{In}_2\text{O}_3$  porous nanoplatelets were obtained.

## 2.3. Characterization and measurements

The phase of the as-synthesized products was characterized using X-ray diffraction (XRD, Shimadzu XRD-6000) with Cu K $\alpha$  radiation ( $\lambda = 1.5406 \text{ \AA}$ ) at a scanning rate of 4° min<sup>-1</sup>. The X-ray tubes were operated with electric current of 30 mA and voltage of 40 kV. The composition, morphology, and size of the products were examined by scanning electron microscopy (SEM, JSM-6480) and transmission electron microscopy (TEM, JEOL-2100). Samples for TEM observation were prepared by dropping the products on a carbon-coated copper grid after ultrasonic dispersion in absolute ethanol. The band gap of the product was determined by ultraviolet–visible (UV–vis) spectroscopy (Shimadzu UV-4100). Raman spectrum was performed at room temperature using a SPEX-1403 Raman spectrometer with 514.5 nm excitation source from an Ar<sup>+</sup> laser.

## 2.4. Fabrication and measurement of $\text{In}_2\text{O}_3$ gas sensor

The gas-sensing properties were measured using a WS-30A gas sensor measurement system (Weisheng Instruments Co., Zhengzhou, China). The gas sensor was fabricated as follows: the  $\text{In}_2\text{O}_3$  samples were mixed with terpineol binder to form a slurry through milling, and then pasted on to a ceramic tube (2 mm in diameter) to form a thin film between two Au electrodes (electrode distance 5 mm), which were previously printed on the ceramic tube and were connected with four platinum wires (Fig. 1). Given amounts of test gases were injected into the testing chamber by a micro-syringe. The humidity in the testing chamber is 25–35% relative humidity at room temperature (22–28 °C). Gas-sensing measurements were carried out at the working temperature of 200 °C, which can be controlled by adjusting the heating voltage ( $V_{\text{heating}}$ ) across a resistor inside the ceramic tube. A reference resistor is put in series with the sensor to form a complete measurement

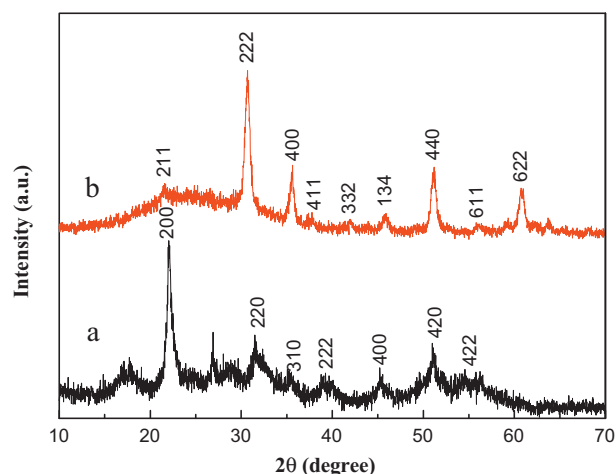


**Fig. 2.** X-ray diffraction patterns of the samples: (a) before calcination and (b) after calcination.

circuit (Fig. 1). In the test process, a working voltage ( $V_{\text{working}}$ ) was applied. By monitoring the voltage ( $V_{\text{output}}$ ) across the reference resistor, the response of the sensor in air or in a test gas could be measured. The gas sensing response is defined as the ratio of the stationary electrical resistance of the sensor in air ( $R_{\text{air}}$ ) to the resistance in the test gas ( $R_{\text{gas}}$ ), i.e.,  $R = R_{\text{air}}/R_{\text{gas}}$ .

## 3. Results and discussion

The phases of the obtained products were firstly determined by XRD. The XRD pattern of the sample before calcination shows several diffraction peaks (Fig. 2a), which can be indexed to cubic phase  $\text{In}(\text{OH})_3$  (JCPDS no. 16-0161). This indicates that this solvothermal process cannot generate pure phase  $\text{In}_2\text{O}_3$ , the followed annealing process is necessary to obtain  $\text{In}_2\text{O}_3$  nanostructures. As shown in Fig. 2b, the XRD pattern of the calcinated sample can be readily indexed to cubic structure  $\text{In}_2\text{O}_3$  with lattice constants  $a = 10.0875 \text{ \AA}$ , which well agrees with the standard value for bixbyite-type cubic  $\text{In}_2\text{O}_3$  (JCPDS card no. 06-0416,  $a = 10.118 \text{ \AA}$ ). The main peaks at 21.6°, 30.7°, 35.6°, 51.2° and 61.0° correspond to the (2 1 1), (2 2 2), (4 0 0), (4 4 0) and (6 2 2) lattice plane of cubic  $\text{In}_2\text{O}_3$ , respectively.

Fig. 3a shows a SEM image of the as-prepared  $\text{In}(\text{OH})_3$  sample. It can be observed that the sheet nanostructures, like curly thin paper, corrugate into a lacery shape, closely associate with each other forming a disordered solid. The corresponding TEM image is shown in Fig. 3b, which clearly indicates that the as-prepared  $\text{In}(\text{OH})_3$  sample is composed of sheet-like nanostructure with side length of about 100–200 nm.

Many metal oxides can be prepared by direct calcination of the corresponding metal hydroxide in air without morphology change. Similar to other metal hydroxides, indium hydroxide can dehydrate to form indium oxides with the same morphology upon heating. Through this route, various  $\text{In}_2\text{O}_3$  nanostructures have been prepared, for example,  $\text{In}_2\text{O}_3$  nanocubes, and microflowers [18]. In our case, porous  $\text{In}_2\text{O}_3$  nanoplatelets were prepared by direct calcination of the  $\text{In}(\text{OH})_3$  sheet-like nanostructures in air at 350 °C for 3 h. Fig. 4a shows the SEM image of the obtained  $\text{In}_2\text{O}_3$  nanoplatelets. It can be seen that the  $\text{In}_2\text{O}_3$  sample is actually composed of numerous nanoplatelets that are randomly arranged to form anomalous aggregates. The thickness of the nanoplatelets is less than 6 nm. A further investigation of the  $\text{In}_2\text{O}_3$  products was made by TEM observation. Fig. 4b shows a typical TEM image of  $\text{In}_2\text{O}_3$  nanoplatelets, from which the side length of the nanoplatelets is determined to be about 20–50 nm. Interestingly, the  $\text{In}_2\text{O}_3$  nanoplatelets show

Download English Version:

<https://daneshyari.com/en/article/744139>

Download Persian Version:

<https://daneshyari.com/article/744139>

[Daneshyari.com](https://daneshyari.com)